

## Theory of X-ray microcomputed tomography in dental research: application for the caries research

Young-Seok Park<sup>1</sup>, Kwang-Hak Bae<sup>2</sup>, Juhea Chang<sup>3</sup>, Won-Jun Shon<sup>4\*</sup>

<sup>1</sup>Department of Oral Anatomy, <sup>2</sup>Department of Preventive and Public Health Dentistry, Seoul National University School of Dentistry and Dental Research Institute, <sup>3</sup>Clinic for Persons with Disabilities, Seoul National University Dental Hospital, <sup>4</sup>Department of Conservative Dentistry, Seoul National University School of Dentistry and Dental Research Institute, Seoul, Korea

### ABSTRACT

Caries remains prevalent throughout modern society and is the main disease in the field of dentistry. Although studies of this disease have used diverse methodology, recently, X-ray microtomography has gained popularity as a non-destructive, 3-dimensional (3D) analytical technique, and has several advantages over the conventional methods. According to X-ray source, it is classified as monochromatic or polychromatic with the latter being more widely used due to the high cost of the monochromatic source despite some advantages. The determination of mineral density profiles based on changes in X-ray attenuation is the principle of this method and calibration and image processing procedures are needed for the better image and reproducible measurements. Using this tool, 3D reconstruction is also possible and it enables to visualize the internal structures of dental caries. With the advances in the computer technology, more diverse applications are being studied, such automated caries assessment algorithms. [J Kor Acad Cons Dent 2011;36(2):98-107.]

**Key words:** Caries diagnosis; Dental caries, Micro-CT; X-ray microcomputed tomography

-Received 19 January 2011; revised 28 January 2011; accepted 1 March 2011-

### INTRODUCTION

Dental caries, a chronic infectious disease, affects more than 90 percent of all adults in the United States<sup>1,2</sup> and over 80 percent of all adults in Korea.<sup>3</sup> Historically, caries have been prevalent since the time of pre-Neolithic humans (10,000 BC) with a reported prevalence between 1.4% and 12.1% cari-

ous teeth, but it was not until the fourteenth and fifteenth century when a sharp increase in caries prevalence was noted.<sup>4</sup> This increase is often ascribed to a sucrose-civilization-caries trinity, with caries prevalence rising above 25%. Interestingly, as sucrose consumption increased, so did the life expectancy.<sup>5</sup>

An understanding of the dental caries process and

<sup>1</sup>Park YS, DDS, MSD, PhD, Assistant Professor; Department of Oral Anatomy

<sup>2</sup>Bae KH, PhD, Associate Professor; Department of Preventive and Public Health Dentistry

<sup>3</sup>Chang JH, DDS, MSD, PhD, Clinical Assistant Professor; Clinic for Persons with Disabilities, Seoul National University Dental Hospital

<sup>4</sup>Shon WJ, DDS, MSD, PhD, Assistant Professor; Department of Conservative Dentistry, Seoul National University School of Dentistry and Dental Research Institute, Seoul, Korea

\*Correspondence to Won-Jun Shon, DDS, MSD, PhD.

Assistant Professor, Department of Operative Dentistry, Seoul National University School of Dentistry, 28 Yeongeon-dong, Jongno-gu, Seoul, Korea, 110-749

TEL, +82-2-2072-2659; FAX, +82-2-2072-3859; E-mail, endoson@snu.ac.kr

\*This research was supported by Basic Science Research Program through the National Research Foundation of Korea (NRF) funded by the Ministry of Education, Science, and Technology (2010-0023586).

management strategies have been advanced through numerous studies.<sup>6</sup> Modern evidence reveals that there is a continuum of disease states ranging from subclinical, subsurface changes to more advanced, clinically detectable subsurface caries, to various stages of more advanced lesions with microscopic and later macroscopic cavitations of the enamel and significant involvement of dentin.<sup>7,8</sup> Therefore, dental caries is more of a “cavity” than a disease process.<sup>9</sup> From a microscopic perspective, the process of caries in dental hard tissues is complex and dynamic, involving a balance between demineralization and remineralization, influenced by the nature of the biofilm environment coating these surfaces.<sup>10</sup> Our understanding of these processes has thus far been limited by the alteration of specimens that results from the techniques used to examine them. Such techniques have included complicated, often destructive methods such as chemical analyses, cross-sectional microhardness determinations (nano-indentation), polarized light microscopy, microprobe analysis, iodine absorptiometry, electrical conductivity studies, and X-ray microtomography.<sup>11</sup>

Computed tomography (CT), invented by Hounsfield in 1973, is a well-known medical technique for the nondestructive examination of internal structures.<sup>12</sup> X-ray microtomography (XMT) is a miniaturized version of CT that has a resolution of microns as opposed to millimeters.<sup>13</sup> Although Elliott and Dover are known to be the inventors of the first XMT in 1982,<sup>14-16</sup> some authors reported that the simplest prototype of the microtomographic scanner emerged in the 1970s and comprised a pinhole collimator and a single detector.<sup>17</sup> For this first generation microtomographic scanner, energy discriminating detection can easily be used, and the attenuation coefficient can be measured using monochromatic radiation, so the mass density of the material the X-rays have penetrated can be determined. However, the data acquisition time for a single slice can take as long as several hours, which limits its use.

The linear-array system is the second generation of microtomographic scanners and has a linear detector array to collect one whole projection at a time. This makes data collection much faster than the single detector system. In this type of system, the X-rays

fan out from the source to the detector and as a result, it is called “fan-beam projection”. Due to the use of a polychromatic X-ray resource, artifacts such as beam hardening can influence its accuracy in quantitative measurements and 3D reconstruction. Therefore, beam hardening correction is an important issue that needs to be considered.

The third generation of microtomographic scanners is an area-array system with a two-dimensional detector array. The X-rays form a cone that produces projections that can be used to reconstruct a 3D image of the specimen. This system is also known as a cone-beam microtomographic scanner. It has the shortest data collection time, but its 3D reconstruction is more complicated than the fan-beam system.<sup>18</sup>

Microcomputed tomography allows for images of internal features to be constructed entirely upon their X-ray attenuation coefficients and enables the investigation of small samples at a resolution of a few micrometers. Nowadays, XMT has emerged as one of the non-destructive 3D analytical techniques in hard tissue research and has been used in various fields of dentistry including caries research.<sup>19-22</sup>

This paper builds on the findings of several recent articles related to caries research using microcomputed tomography, and seeks to outline the current research status and future trends of advanced applications.

### Comparisons with conventional methodologies

Among various experimental methods, the conventional gold-standard in *in vitro* caries studies is histological assessment by expert examiners of either hemi- or serial sections cut from the tooth, and transverse micro-radiography (TMR), where thin slices of the tooth are X-rayed to determine their mineral density. The latter has been a widely accepted method for determining mineral loss or gain in experimentally induced incipient carious lesions<sup>17</sup> and has been used for the comparison and validation of other newly developed caries detection techniques.<sup>23-25</sup> Both of these methods require the tooth to be sectioned as thin as 100  $\mu\text{m}$ , which introduces a variation in the results and prevents the longitudinal analysis or assessment of teeth by an examiner.

Furthermore, the location of the original surface of a dentinal lesion may be hard to determine because air drying dentinal lesions can result in characteristic surface shrinkage.<sup>26</sup>

Polarized light microscopy (PLM), another widely used method, is a very laborious procedure, but is less expensive than TMR and can give an accurate measurement of lesion depth even though it is usually used as a qualitative method.<sup>27</sup> Conventional microscopy methods such as contact microradiography and scanning microscopy (e.g., confocal microscopy and back-scattered scanning electron microscopy) are usually 2-dimensional (2D) and also involve destruction of the sample. These methods are only able to examine lesions at one point in time, either before or after experimental procedures are carried out on the samples.

As a nondestructive method, XMT can offer a potential solution to the problem that the previously mentioned methodologies have.<sup>28</sup> Since there is no physical sectioning using XMT, there is no loss of information between sections, and repeated scans that allow for the comparison of the same sample before or after experiments are possible.<sup>18,29</sup> The scarcity of suitable sample is no longer a major burden when this method is used instead of other destructive methods.<sup>30</sup>

In addition, XMT aims to create a 3D dataset representing the radiopacity at every point within a sample, and the analysis of this 3D dataset allows for reconstruction of the volumetric data.<sup>31</sup> The creation of this type of dataset is impossible with the conventional methods. Since XMT produces a full 3D X-ray attenuation map of the scanned object, there is no compression of 3D information into two dimensions, i.e., the resultant image is a true representation with no superimposition, as in intraoral radiographs. These advantages have made XMT more popular as a means of measuring demineralization *in vitro*.<sup>32,33</sup> Since radiopacity corresponds well to mineral density in teeth, XMT is well-suited in detecting demineralization characteristics of caries lesions.<sup>34</sup> Furthermore, the nature of the data obtained in XMT lends itself to automated analysis.<sup>28</sup>

## Two types of microcomputed tomography and artifacts

Different types of XMT systems are used for caries research.<sup>35</sup> The difference between these types of XMT systems is based on the different X-ray sources, e.g., monochromatic or polychromatic, different target materials, synchrotron with a single crystal monochromator<sup>36</sup>, or in the different ways of shadow image detection, such as selective photon counting or using a Charge Couple Device (CCD) camera with a scintillator.<sup>16,37</sup> In the case of polychromatic set-ups, the relationship between the attenuation and material thickness is nonlinear. Indeed, lower-energy X-rays in the beam are more strongly absorbed than higher-energy X-rays, and as a result, the energy distribution spectrum of the beam changes as it passes through the object. The outgoing beam contains a higher proportion of high energy (or "hard") X-rays. In other words, the beam becomes harder, and this phenomenon is called beam hardening. The beam hardening effect can result in severe artifacts that can degrade the quality of the CT images.<sup>38,39</sup> Polychromatic systems have already been used in caries research,<sup>37</sup> but the assessments of the quality-degrading effect of beam hardening and its possible correction is still being studied.

Monochromatic (synchrotron) radiation has successfully been used as an X-ray source in XMT studies to volumetrically determine the mineral concentration in sound and carious enamel/dentin.<sup>38,39</sup> However, the high cost and low availability of these synchrotron sources still impairs its widespread use. There have been several reports, including Dowker et al., that utilize a synchrotron XMT.<sup>39-41</sup>

Today, commercially available desktop XMT systems make use of polychromatic X-ray sources, which unfortunately introduce scanning artifacts such as beam hardening and loss of information due to energy averaging (Figure 1).<sup>42,43</sup> Beam-hardening artifacts arise from polychromatic sources because the attenuation of the incident X-ray beam is not exponentially related to the thickness of the object, as predicted by Beer's law.<sup>44,45</sup> The lower X-ray energies of the polychromatic spectrum are thus easily absorbed, while the higher energies are less attenuated. This results in a higher brightness rim around the edge of the

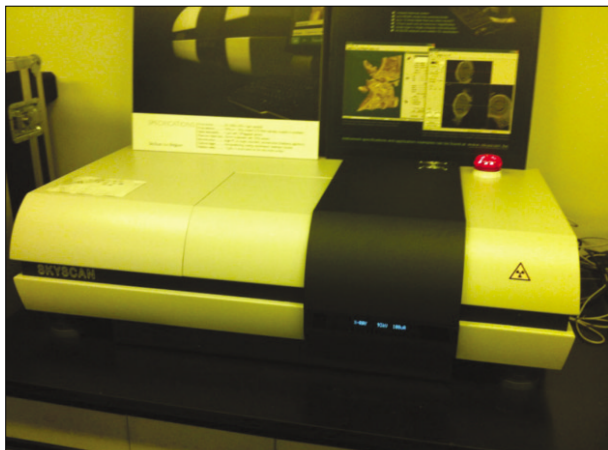


**Figure 1.** Example of desktop polychromatic X-ray microtomography, Skyscan 1172 (Skyscan, Kontich, Belgium).

cross-sectioned image of the object, possibly combined with scattering of the background in the projection area (“cupping” artifacts).<sup>46</sup> Therefore, the resulting intensities produced in the X-ray projection images are not necessarily proportional to the object thickness if this artifact is not corrected. When studying caries, this artifact may impair the quantitative analysis of mineral concentration and compromise the segmentation of structures with different gray-value peaks in the histogram.

Scattering is another important source of artifacts in CT images, especially when cone-beam geometry is applied, as in the case of XMT. Scattering, like beam hardening, induces nonlinear errors in the measurement of attenuation values, which can lead to “cupping” in homogeneous objects or dark streaks between image regions of high attenuation.<sup>42,44</sup> The scattering effect can be a more significant source of error for large objects, and it was shown that the artifact propensity is a direct function of the scatter-to-primary radiation ratio.<sup>47,48</sup>

### Measurements and calibrations

Generally, the most frequently defined parameter which we would like to acquire in caries research is the mineral density of the tooth structure or its change from a specific site.<sup>35</sup> The determination of mineral density profiles is based on changes in X-ray

attenuation. It has been shown that a linear relationship between the X-ray attenuation coefficient and mineral density exists, and the grey levels of the reconstructed XMT slices correspond directly to a map of the attenuation coefficients within a sample.<sup>49,50</sup> Using the linear attenuation coefficient (LAC) obtained from an XMT scan as the parameter that represents the mineral density of the dental hard tissues makes the measurement process and handling of data simpler. The LAC describes the extent to which the intensity of an energy beam is reduced as it passes through a specific material.<sup>17</sup> A small LAC value indicates that the material to be tested is relatively transparent, while larger values indicate greater degrees of opacity. Generally, the higher the energy of the radiation and the less dense the material, the lower the corresponding LAC will be. Since the minerals in dental tissues (mainly hydroxyapatite) are responsible for most of the X-ray attenuation observed in caries studies, and normal variations in the chemical composition of enamel minerals have little effect on the LAC, a variation in the LAC for enamel is proportional to its mineral density.<sup>16,19,40,41,49,51</sup> Dentin is composed of approximately 35% organic substances by weight, mainly collagen. Collagen’s contribution to the total X-ray attenuation coefficient in dentin is around 5% at an energy of 25 keV. Thus, a variation in the dentin LAC can be considered proportional to dentin mineral density,<sup>34</sup> although there are controversies about this assumption as discussed below.<sup>37</sup> The mineral content of teeth can be measured with an accuracy better than 1% with a resolution between 5 and 30  $\mu\text{m}$  using monochromatized XMT.<sup>35</sup>

It is important that some form of calibration is used with XMT systems to validate the quantitative information obtained from different machines.<sup>10</sup> A number of researchers have looked at the issue of creating calibration standards, also known as “phantoms”, for application when studying dental hard tissues. Commercially produced phantoms are available, but are relatively expensive. Phantoms may be fabricated from various materials such as pure aluminium wire or post with diverse dimensions<sup>17,35</sup>, but ideally, phantoms should be composed of materials that relate to the examined tissues.

Since the main mineral component present in dental enamel and dentin is hydroxyapatite (HAP), pure crystalline HAP approximates the composition of enamel and thus can be used as a representation of enamel. Pure powdered HAP, when sintered, forms spatially homogeneous solid crystalline structures<sup>32,52,53</sup>, but their manufacture is limited to densities above about 1.4 g/cm<sup>3</sup> in practical applications.<sup>53</sup> Difficulties are encountered when the creation of robust, dimensionally stable and reliable HAP phantoms with very low mineral concentrations is attempted. HAP is relatively hydrophobic and poorly soluble, and as a result, this has led some researchers to investigate other more stable materials such as dipotassium hydrogen phosphate (K<sub>2</sub>HPO<sub>4</sub>)<sup>54-57</sup> and lithium tetraborate (Li<sub>2</sub>B<sub>4</sub>O<sub>7</sub>).<sup>52</sup> Unfortunately, these materials pose a disadvantage in that they are not found naturally in dental hard tissues, and designs of phantoms using these materials ignore the organic phase and water present in hard tissues.

In contrast to enamel, calibrating a laboratory XMT system for mineral density determination of dentin remains a major challenge.<sup>54</sup> The reported densities of sound enamel range between 2.65 and 2.89 g/cm<sup>3</sup>.<sup>16,32,40,41,58-60</sup> The densities of dentin have been estimated to be between 1.46 g/cm<sup>3</sup> for incisors and 1.62 g/cm<sup>3</sup> for molars,<sup>18,58</sup> with circumpulpal dentin having a lower density (1.3 g/cm<sup>3</sup>) than peripheral dentin (1.5 g/cm<sup>3</sup>). The average mineral concentration of sound human dentin has been measured at 1.29 g/cm<sup>3</sup>, with demineralized dentin being only 0.55 g/cm<sup>3</sup>.<sup>34</sup> Remineralized dentin exhibits a significantly higher mineral concentration (2.25 g/cm<sup>3</sup>) when measured using synchrotron-generated X-radiation.<sup>34</sup>

Demineralized bone has been studied for creating phantoms to mimic the non-crystalline organic component of bone.<sup>61</sup> However, bone is a complicated material that is composed of HAP, collagen, and marrow tissue crystalline and organic fractions. Some researchers assume that X-ray absorption in the demineralized portion of bone is constant.<sup>62</sup> Similar assumptions can be made about the demineralized portion of dentin. Resin has been used by several authors as a soft tissue equivalent for the fabrication of radiographic phantoms,<sup>55,63-65</sup> but the non-uniform

distribution of powder during the mixing and resin curing processes<sup>66</sup> has resulted in grainy radiographic images. Recently, Schwass et al. introduced the mixture of unfilled resin and hydroxyapatite as a phantom that mimics dentin. Currently, there seems to be no consensus or standard in calibration methods.

### Data processing and 3-dimensional reconstruction

The data acquired from XMT studies cannot be used as raw data; pre- or post-processing procedures are usually required. These kinds of processing make it impossible to compare or correlate the results of XMT studies because of the methodological differences in measuring the mineral-density values.<sup>67</sup> Aside from the calibration or phantoms mentioned above, when using XMT in longitudinal or case-control studies, it is of primary importance to standardize the scanning and reconstruction parameters for each tooth and to adequately correct for polychromatic artifacts.

Some correction methods for beam-hardening artifacts have been recommended during either the acquisition or the reconstruction phase. The classical approach to pre-processed XMT slices of structures deeply affected by beam-hardening or "cupping" artifacts is to first apply an initial conservative threshold. This would segment both the desired structure and the background. Access to the synchrotron sources of monochromatic radiation to avoid this effect is not really practical. Their accuracy is better when higher-energy X-rays are used. The noise increases with decreased energy since low-energy soft X-rays scatter and penetrate less efficiently than hard X-rays.<sup>66</sup> The inadequate filtration of soft radiation leads to a non-linear photon count versus object thickness detector responses. By placing a filter (e.g., aluminum) between the X-ray source and the object during the acquisition phase, the low-energy X-rays can be attenuated as a consequence of the photoelectric effect. This is necessary to limit the spectral bandwidth of X-rays and increase the accuracy of the beam-hardening correction. However, since this method results only in the reduction of the beam-hardening effect, it is commonly used in conjunction with other correction schemes.<sup>68</sup> During the reconstruction phase, the measured nonlinear relationship

between the attenuation and the material thickness can be linearized based on a calibration curve. Using this complimentary methodology, beam-hardening artifacts can be corrected if the specimen is made of either one phase or several phases with attenuation coefficients that differ by a near-constant factor across the energy spectrum used.<sup>45,69,70</sup> These beam-hardening correction schemes that are applied during the reconstruction phase can lead to a noise increase in the cross-section slices.<sup>69,70</sup>

Energy-based beam hardening correction was used to convert the polychromatic energy data into monochromatic data,<sup>69,70</sup> but this process introduced some noise. The presence of noise is also inversely related to the resolution used during the scanning procedure. Resolution is directly related to the scanning time and the computer resources needed, and is inversely related to the size of the scanned field.<sup>45</sup> In fact, noise will be inherently present in any XMT slices, especially if reasonably short scanning times are used (less than 1 hour).<sup>71,72</sup>

Flat-field correction was used to reduce the ring artifact effects.<sup>69,73</sup> Flat-field correction is a commonly used approach for the problem to remove artifacts from 2D images that are caused by variations in the pixel-to-pixel sensitivity of the detector or by distortions in the optical path. The ring artifacts are caused by imperfect detector elements, which throughout the scan process significantly under- or overestimate attenuation values. It is noted in the reconstructed image as concentric ring-like shape. Frame averaging was used to reduce the noise of each projection, increasing the signal-to-noise ratio, but the trade-off was that scan times were increased.<sup>54</sup> A Gaussian filter was applied to reduce the background noise, thereby reducing the signal-to-noise ratio while leaving the mineral density information intact.<sup>32</sup>

Most commercial XMT systems have analytic reconstruction software based on the Feldkamp algorithm. Despite important progress in exact reconstruction algorithms,<sup>74</sup> the approximate methods remain practically important, and among them, the Feldkamp algorithm is the most popular.<sup>75</sup> The main advantages of this reconstruction algorithm are the possibility of using incomplete scanning loci, partial

detection coverage, and their high computational efficiency. From a technical point of view, the single-circular scan path, in which the X-ray source rotates in a plane around the subject, is often the only feasible path with isocentric rotational machines. In situations like these, Feldkamp algorithm reconstruction methods are preferred. However, iterative reconstruction formulas such as the maximum likelihood algorithm are better able to reduce noise according to Chueh et al.<sup>65</sup>

### Problems to be solved

Because XMT enables 3D imaging of internal structures, several recent papers have dealt with the 3D quantitative evaluation of dental caries.<sup>29,37,60</sup> Qualitative volume rendering based on XMT slices of a primary carious tooth has been previously described.<sup>13</sup> Later, the volume of carious and sound dentin removed by a conventional carbide bur was quantitatively determined,<sup>37</sup> confirming the applicability of XMT in volumetric measurement of caries excavation. However, such studies still involved time-consuming scanning and reconstruction procedures, and some methodological aspects were not clearly described.<sup>67</sup> These kinds of studies used the radiopacity threshold to identify lesions. The working principle of the radiopacity threshold is based on a mathematical reconstruction of the LAC of each spot into a cross-sectional slice through an object (which is a function of its elemental composition and density/concentration) measured by a series of X-ray projections.<sup>15</sup> Traditionally, thresholding is accomplished by defining a range of brightness values in the original image, selecting the pixels within this range as belonging to the foreground, and rejecting all of the other pixels as belonging to the background. Such an approach has been successful when previously applied for sound enamel and dentin.<sup>76</sup> In more difficult cases, however, the brightness levels of individual pixels are not uniquely related to the desired structure,<sup>72</sup> as is the case for carious enamel and dentin. Earlier works on 3D rendering of a carious tooth mentioned that beyond the difficulties in distinguishing carious enamel and dentin, no adequate threshold for the boundary between sound and cari-

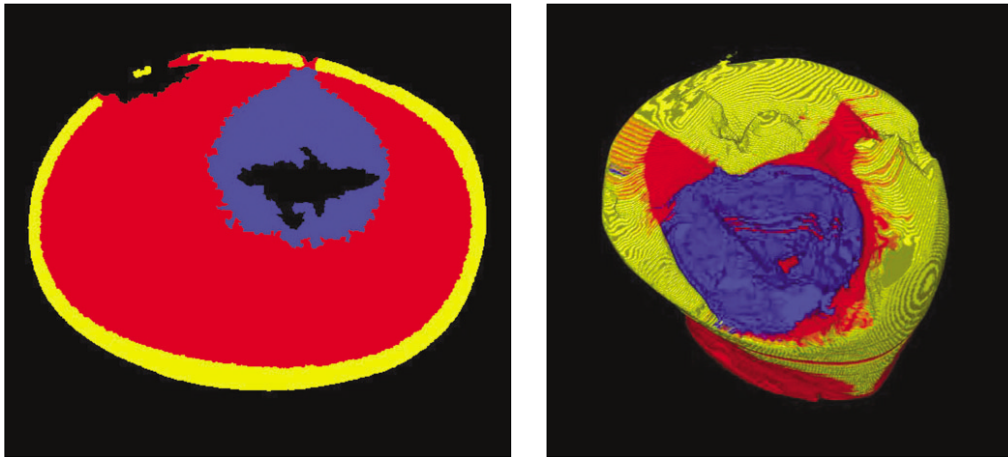


**Figure 2.** 3-dimensional rendering of carious tooth (the results of pilot study of the authors).

ous dentin has yet been defined.<sup>13</sup> The pilot study performed by the authors confirmed these difficulties (Figure 2).

Inconsistent mineral density in the individual tooth structures of enamel and dentin is another difficulty in establishing reliable boundaries. The partial volume effects that would arise when a single pixel or voxel contains both the structure of interest and the background<sup>77,78</sup> must be considered because its effect directly increases with pixel size (reduction in spatial resolution).

Recently, an automated algorithm for caries research was reported.<sup>28</sup> Adequate segmentation of structures with overlapping gray values may require cluster-threshold algorithms in the near future (as computer power continues to increase). Such techniques are supposed to be based not only on gray values or voxel connectivity, but are also supposed to take into account differences in texture or distance maps between candidate regions of sound and carious dentin.

### CONCLUSIONS

In this article, the general features of XMT and its usage in caries research was widely reviewed. As a nondestructive analytical tool, XMT has been widely used in various fields of dentistry. The difference or change in mineral density is the basis of hard tissue research, and the more practical and accurate approach with XMT compared to conventional meth-

ods has allowed for its greater usage in the field of caries research.

The ability to render 3D images enabled unprecedented analysis; however, the standardization of the research protocol is imperative for this method. It is expected that a more expanded application of XMT is possible through further study with rapid advances in 3D technologies such as CAD-CAM in parallel.

### REFERENCES

1. Kaste LM, Selwitz RH, Oldakowski RT, Brunelle JA, Winn D, Brown L. Coronal caries in the primary and permanent dentition of children and adolescents 1-17 years of age: United States, 1988-1991. *J Dent Res* 1996; 75(spec issue):631-641.
2. Winn DM, Brunelle JA, Selwitz RH, Kaste LM, Oldakowski RJ, Kingman A, Brown LJ. Coronal and root caries in the dentition of adults in the United States, 1988-1991. *J Dent Res* 1996;75(spec issue): 642-651.
3. Ministry of Health and Welfare. National survey of oral health in 2006. Seoul, Korea Ministry of Health and Welfare.
4. Fontana M, Young DA, Wolff MS, Pitts NB, Longbottom C. Defining dental caries for 2010 and beyond. *Dent Clin North Am* 2010;54:423-440.
5. Keene HJ. "History of dental caries in human populations: the First Million Years" animal models in cariology. In: Tanzer JM, editor. Proceedings, Animal Models in Cariology. Washington, DC: *Information Retrieval Inc* 1981:23-40.
6. Bader JD, Shugars DA, Bonito AJ. Systematic reviews of selected dental caries diagnostic and management methods. *J Dent Educ* 2001;65:960-968.
7. Featherstone JD. The continuum of dental caries-evidence for a dynamic disease process. *J Dent Res* 2004; 83(Spec Iss C):C39-C42.

8. Kidd EA, Fejerskov O. What constitutes dental caries? histopathology of caries enamel and dentin related to the actions of cariogenic biofilms. *J Dent Res* 2004;83(Spec Iss C): C35-C38.
9. Pitts NB. Modern concepts of caries measurement. *J Dent Res* 2004;83(Spec Iss C):C43-C47.
10. Schwass DR, Swain MV, Purton DG, Leichter JW. A system of calibrating microtomography for use in caries research. *Caries Res* 2009;43:314-321.
11. de Josselin De Jong E, Sundström F, Westerling H, Tranaeus S, ten Bosch JJ, Angmar-Månsson B. A new method for in vivo quantification of changes in initial enamel caries with laser fluorescence. *Caries Res* 1995;29:2-7.
12. Hounsfield GN. Computerized transverse axial scanning (tomography). 1. Description of system. *Br J Radiol* 1973;46:1016-1022.
13. Wong FS, Willmott NS, Davis GR. Dentinal carious lesion in three dimensions. *Int J Paediatr Dent* 2006;16:419-423.
14. Elliott JC, Dover SD. X-ray microtomography. *J Microsc* 1982;126:211-213.
15. Elliott JC, Davis GR, Anderson P, Wong FSL, Dowker SEP, Mercer CE. Application of laboratory microtomography to the study of mineralised tissues. *Anal Quim* 1997;93:77-82.
16. Wong FSL, Anderson P, Fan H, Davis GR. X-ray microtomographic study of mineral concentration distribution in deciduous enamel. *Arch Oral Biol* 2004;49:937-944.
17. Lo EC, Zhi QH, Itthagaran A. Comparing two quantitative methods for studying remineralization of artificial caries. *J Dent* 2010;38:352-359. Epub 2010 Jan 14.
18. Davis GR, Wong FS. X-ray microtomography of bones and teeth. *Physiol Meas* 1996;17:121-146.
19. Efeoglu N, Wood DJ, Efeoglu C. Thirty-five percent carbamide peroxide application causes in vitro demineralization of enamel. *Dent Mater* 2007;23:900-904.
20. Engelke K, Graeff W, Meiss L, Hahn M, Delling G. High spatial resolution imaging of bone mineral using computed microtomography. Comparison with microradiography and undecalcified histologic sections. *Invest Radiol* 1993;28:341-349.
21. Park YS, Yi KY, Lee IS, Jung YC. Correlation between microtomography and histomorphometry for assessment of implant osseointegration. *Clin Oral Implants Res* 2005;16:156-160. Erratum in: *Clin Oral Implants Res* 2005;16:258.
22. Park YS, Yi KY, Lee IS, Han CH, Jung YC. The effects of ion beam-assisted deposition of hydroxyapatite on the grit-blasted surface of endosseous implants in rabbit tibiae. *Int J Oral Maxillofac Implants* 2005;20:31-38.
23. Lee C, Darling CL, Fried D. Polarization-sensitive optical coherence tomographic imaging of artificial demineralization on exposed surfaces of tooth roots. *Dent Mater* 2009;25:721-728.
24. Hsu DJ, Darling CL, Lachica MM, Fried D. Nondestructive assessment of the inhibition of enamel demineralization by CO<sub>2</sub> laser treatment using polarization sensitive optical coherence tomography. *J Biomed Opt* 2008;13:054027.
25. Manesh SK, Darling CL, Fried D. Nondestructive assessment of dentin demineralization using polarization-sensitive optical coherence tomography after exposure to fluoride and laser irradiation. *J Biomed Mater Res B Appl Biomater* 2009;90:802-812.
26. Wefel JS, Heilman JR, Jordan TH. Comparisons of in vitro root caries models. *Caries Res* 1995;29:204-209.
27. Ten Bosch JJ, Angmar-Månsson B. A review of quantitative methods for studies of mineral content of intra-oral caries lesions. *J Dent Res* 1991;70:2-14.
28. Taylor AM, Satterthwaite JD, Ellwood RP, Pretty IA. An automated assessment algorithm for micro-CT images of occlusal caries. *Surgeon* 2010;8:334-340.
29. Hahn SK, Kim JW, Lee SH, Kim CC, Hahn SH, Jang KT. Microcomputed tomographic assessment of chemomechanical caries removal. *Caries Res* 2004;38:75-78.
30. Huysmans MC, Longbottom C. The challenges of validating diagnostic methods and selecting appropriate gold standards. *J Dent Res* 2004;83:C48-C52.
31. Flannery BP, Deckman HW, Roberge WC, D'Amico KL. Three-dimensional X-ray microtomography. *Science* 1987;237:1439-1444.
32. Huang TT, Jones AS, He LH, Darendeliler MA, Swain MV. Characterisation of enamel white spot lesions using x-ray micro-tomography. *J Dent* 2007;35:737-743.
33. Efeoglu N, Wood D, Efeoglu C. Microcomputerised tomography evaluation of 10% carbamide peroxide applied to enamel. *J Dent* 2005;33:561-567.
34. Kinney JH, Marshall GW Jr, Marshall SJ. Three-dimensional mapping of mineral densities in carious dentin: theory and method. *Scanning Microsc* 1994;8:197-205.
35. Kovács M, Danyi R, Erdélyi M, Fejérdy P, Dobó-Nagy C. Distortional effect of beam-hardening artefacts on microCT: a simulation study based on an in vitro caries model. *Oral Surg Oral Med Oral Pathol Oral Radiol Endod.* 2009;108:591-599.
36. Kinney JH, Balooch M, Haupt DL Jr, Marshall SJ, Marshall GW Jr. Mineral distribution and dimensional changes in human dentin during demineralization. *J Dent Res* 1995;74:1179-1184.
37. Willmott NS, Wong FS, Davis GR. An X-ray micro tomographystudy on the mineral concentration of carious dentine removed during cavity preparation in deciduous molars. *Caries Res* 2007;41:129-134.
38. van de Castele E, Van Dyck D, Sijbers J, Raman E. An energy-based beam hardening model in tomography. *Phys Med Biol* 2002;47:4181-4190.
39. Dowker SE, Davis GR, Elliott JC. X-ray microtomography: nondestructive three dimensional imaging for in vitro endodontic studies. *Oral Surg Oral Med Oral Pathol Oral Radiol Endod* 1997;83:510-516.
40. Dowker SE, Elliott JC, Davis GR, Wassif HS. Longitudinal study of the three-dimensional development of subsurface enamel lesions during in vitro demineralisation. *Caries Res* 2003;37:237-245.
41. Dowker SE, Elliott JC, Davis GR, Wilson RM, Cloetens P. Synchrotron X-ray microtomographic investigation of mineral concentrations at micrometre scale in sound and carious enamel. *Caries Res* 2004;38:514-522.
42. Coljin AP, Zbijewski W, Sasov A, Beckman FJ. Experimental validation of a rapid Monte Carlo based micro-CT simulator. *Phys Med Biol* 2004;49:4321-4333.
43. Sidky EY, Zou Y, Pan X. Impact of polychromatic x-ray sources on helical, cone-beam computed tomography and dual-energy methods. *Phys Med Biol* 2004;49:2293-2303.

44. Kyriakou Y, Kalender WA. X-Ray scatter data for flat-panel detector CT. *Phys Med* 2007;23:3-15.
45. Davis GR, Elliott JC. Artefacts in X-ray microtomography of materials. *Mater Sci Technol* 2006;22:1011-1018.
46. Hammersberg P, Mangard M. Correction for beam hardening artefacts in computerised tomography. *J X-ray Sci Technol* 1998;8:75-93.
47. Joseph PM, Spital RD. The effects of scatter in X-ray computed tomography. *Med Phys* 1982;9:464-472.
48. Malusek A, Seger MM, Sandborg M, Carlsson G. Effect of scatter on reconstructed image quality in cone beam computed tomography: evaluation of a scatter-reduction optimisation function. *Radiat Prot Dosimetry* 2005;144:337-340.
49. Elliott JC, Wong FS, Anderson P, Davis GR, Dowker SE. Determination of mineral concentration in dental enamel from X-ray attenuation measurements. *Connect Tissue Res* 1998;38:61-72. discussion 73-79.
50. Nuzzo S, Lafage-Proust MH, Martin-Badosa E, Boivin G, Thomas T, Alexandre C, Peyrin F. Synchrotron radiation microtomography allows the analysis of three-dimensional microarchitecture and degree of mineralization of human iliac crest biopsy specimens: effects of etidronate treatment. *J Bone Miner Res* 2002;17:1372-1382.
51. Wong FS, Elliott JC. Theoretical explanation of the relationship between backscattered electron and X-ray linear attenuation coefficients in calcified tissues. *Scanning* 1997;19:541-546.
52. Schweizer S, Hattendorf B, Schneider P, Aeschlimann B, Gauckler L, Müller R, Günther D. Preparation and characterization of calibration standards for bone density determination by micro-computed tomography. *Analyst* 2007;132:1040-1045.
53. He LH, Standard OC, Huang TT, Latella BA, Swain MV. Mechanical behaviour of porous hydroxyapatite. *Acta Biomater* 2008;4:577-586.
54. Zou W, Gao J, Jones AS, Hunter N, Swain MV. Characterisation of a novel calibration method for mineral density determination of dentine by X-ray microtomography. *Analyst* 2009;134:72-79.
55. Nuzzo S, Peyrin F, Cloetens P, Baruchel J, Boivin G. Quantification of the degree of mineralization of bone in three dimensions using synchrotron radiation microtomography. *Med Phys* 2002;29:2672-2681.
56. Genant HK, Boyd D. Quantitative bone mineral analysis using dual energy computed tomography. *Invest Radiol* 1977;12:545-551.
57. Cann CE, Genant HK. Precise measurement of vertebral mineral content using computed tomography. *J Comput Assist Tomogr* 1980;4:493-500.
58. Manly RS, Hodge HC, Ange LE. Density and refractive index studies of dental hard tissues. II. Density distribution curves. *J Dent Res* 1939;18:203-211.
59. Clementino-Luedemann TN, Dabanoglu A, Ilie N, Hickel R, Kunzelmann KH. Micro-computed tomographic evaluation of a new enzyme solution for caries removal in deciduous teeth. *Dent Mater J* 2006;25:675-683.
60. Clementino-Luedemann TN, Kunzelmann KH. Mineral concentration of natural human teeth by a commercial micro-CT. *Dent Mater J* 2006;25:113-119.
61. Bowman SM, Zeind J, Gibson LJ, Hayes WC, McMahon TA. The tensile behavior of demineralized bovine cortical bone. *J Biomech* 1996;29:1497-1501.
62. Postnov AA, Vinogradov AV, Van Dyck D, Saveliev SV, de Clerck NM. Quantitative analysis of bone mineral content by X-ray microtomography. *Physiol Meas* 2003;24:165-178.
63. Cheng JC, Qin L, Cheung CS, Sher AH, Lee KM, Ng SW, Guo X. Generalized low areal and volumetric bone mineral density in adolescent idiopathic scoliosis. *J Bone Miner Res* 2000;15:1587-1595.
64. Zheng Y, Lu WW, Zhu Q, Qin L, Zhong S, Leong JC. Variation in bone mineral density of the sacrum in young adults and its significance for sacral fixation. *Spine* 2000;25:353-357.
65. Chueh HS, Tsai WK, Fu HM, Chen JC. Evaluation of the quantitative capability of a homemade cone-beam micro computed tomography system. *Comput Med Imaging Graph* 2006;30:349-355.
66. Bonse U, Busch F, Günnewig O, Beckmann F, Pahl R, Delling G, Hahn M, Graeff W. 3D computed X-ray tomography of human cancellous bone at 8 microns spatial and 10(-4) energy resolution. *Bone Miner* 1994;25:25-38.
67. Neves Ade A, Coutinho E, Vivan Cardoso M, Jacques SV, Van Meerbeek B. Micro-CT based quantitative evaluation of caries excavation. *Dent Mater* 2010;26:579-588. Epub 2010 Mar 29.
68. Brooks RA, Di Chiro G. Beam hardening in X-ray reconstructive tomography. *Phys Med Biol* 1976;21:390-398.
69. Van de casteele E, Van dyck D, Sijbers J, Raman E. A model-based correction method for beam hardening artefacts in X-ray microtomography. *J X-ray Sci Technol* 2004;12:43-57.
70. Van de Castele E, Van Dyck D, Sijbers J, Raman E. The effect of beam hardening on resolution in X-ray microtomography. *Med Imag* 2004;5370:2089-2096.
71. Davis GR. Image quality and accuracy in X-ray microtomography. *Proc SPIE* 1999;3772:147-155.
72. Russ J. The image processing handbook. Boca Raton. *CRC Press* 2007:817.
73. Sijbers J, Postnov A. Reduction of ring artefacts in high resolution micro-CT reconstructions. *Phys Med Biol* 2004;49:N247-N253.
74. Smith BD. Image reconstruction from cone-beam projections: necessary and sufficient condition and reconstruction method. *IEEE Trans Med Imaging* 1985;4:14-25.
75. Wang B, Hong Liub, Shiyong Zhaoc and Ge Wangd Feldkamp-type image reconstruction from equiangular data. *J Xray Sci Technol* 2001;9:113-120.
76. Magne P. Efficient 3D finite element analysis of dental restorative procedures using micro-CT data. *Dent Mater* 2007;23:539-548.
77. Jan J. Medical image processing, reconstruction and restoration: concepts and methods. *New York: Taylor & Francis*; 2006. p710.
78. Dufresne T. Segmentation techniques for analysis of bone by three-dimensional computed tomographic imaging. *Technol Health Care* 1998;6:351-359.

## 국문초록

## 치과 분야 연구에서 미세전산화 단층촬영술의 이론: 치아우식증에 대한 적용

박영석<sup>1</sup> · 배광학<sup>2</sup> · 장주혜<sup>3</sup> · 손원준<sup>4</sup>서울대학교 치의학대학원 <sup>1</sup>구강해부학교실 및 치학연구소, <sup>2</sup>예방치학교실 및 치학연구소<sup>3</sup>서울대학교 치과병원 장애인클리닉, <sup>4</sup>서울대학교 치의학대학원 치과보존학교실 및 치학연구소

치아우식증은 현대 사회에서 여전히 유병률이 높으며, 치과 분야의 주요 상병으로 자리잡고 있다. 치아우식증에 대한 연구에 매우 다양한 방법들이 동원되고 있으나, 최근 미세전산화 단층촬영은 비파괴적인 3차원 분석 기술로서 인기를 얻어 왔으며, 기존의 방법들에 비해 다양한 장점들을 가지고 있다. 미세전산화 단층촬영술은 X선원의 종류에 따라, 모노크로매틱 혹은 폴리크로매틱으로 나뉘어지고, 전자의 경우 몇몇 장점에도 불구하고, 고가의 장비를 요구하므로 후자가 훨씬 널리 사용된다. 투과방사선량의 감소에 따라 결정되는 미네랄 밀도의 차이가 기본 원리이며, 보다 좋은 이미지와 재현 가능한 측정을 위해서는 장비의 교정과 이미지 보정 작업등이 요구된다. 또한, 미세전산화 단층촬영술을 이용하면, 치아우식 병소의 3차원적인 재건이 가능하며, 병소의 내부 구조를 가시화할 수 있다. 최근 컴퓨터 기술의 발전과 더불어 다양한 응용이 시도되고 있는데, 자동화된 충치의 정량적 분석 알고리즘 등이 그 예에 해당된다.

**주요단어:** 마이크로씨티; 미세전산화 단층촬영술; 치아우식증